3B2v7.51c GML4.3.1 VAC : 2586 Prod.Type:COM pp.1–6(col.fig.:NIL) ED:SusanKoshy PAGN: Administrator SCAN: MANGALA

ARTICLE IN PRESS

PERGAMON

Vacuum ▮ (▮▮▮▮) ▮▮▮–▮▮▮

VACUUM
SURFACE ENGINEERING, SURFACE INSTRUMENTATION & VACUUM TECHNOLOGY

www.elsevier.com/locate/vacuum

Kinetics of metastable atoms and molecules in N_2 microwave discharges

V. Guerra*, E. Tatarova, C.M. Ferreira

Centro de Física dos Plasmas, Instituto Superior Técnico, 1049-001 Lisboa, Portugal

Received 15 March 2002; received in revised form 1 April 2002

Abstract

The kinetics of ground-state N(^{4}S) and metastable N(^{2}D) and N(^{2}P) atoms and of the molecular metastable state $N_2(A\ ^3\Sigma_u^+)$ are studied in the framework of a self-consistent model for a nitrogen surface-wave discharge. These species are shown to be strongly coupled under the discharge conditions of this study: field frequency $\omega/2\pi = 2.45$ GHz; gas pressure $p = 267$ Pa. The production and loss mechanisms of each of these species are analysed and discussed in detail.

Keywords: Nitrogen; Discharge; Modelling; Metastables; Kinetics; Atoms

1. Introduction

Metastable particles have long been an important subject of research and keep attracting attention nowadays. As an example, a special issue on metastables and long-lived species recently appeared in J. Phys. D: Appl. Phys. including many articles devoted to the study of the first electronically excited molecular metastable state of nitrogen $N_2(A\ ^3\Sigma_u^+)$ in different conditions [1–7].

Ground-state nitrogen atoms are interesting in many applications, in particular in nitriding processes, which improve the hardness and resistance to corrosion of the surface of different materials [8,9]. Therefore, both theoretical and experimental studies on the production and loss mechanisms of nitrogen atoms are of importance. However, in spite of the large number of measurements and theoretical articles on the subject, dissociation of nitrogen in gas discharges is still not completely understood, in particular in what concerns wall recombination and the role of atomic metastable states, as pointed out in Refs. [10,11] discussed below.

In the previous work, our group has developed theoretical models for nitrogen discharges accounting in a self-consistent way for electron and heavy (neutral and charged) particle kinetics, gas thermal balance and wave electrodynamics and allowing one to determine the axial structure of the discharge. The detailed kinetic scheme for electrons and heavy particles was presented and applied to DC discharges in [10] and to a homogeneous surface-wave discharge in Ref. [12]; the coupling with the wave electrodynamics in a surface-wave discharge was made in Ref. [13], while the gas thermal balance equation was further

*Corresponding author. Fax: +351-21-846-44-57.
E-mail address: vguerra@theta.ist.utl.pt (V. Guerra).

0042-207X/02/$ - see front matter © 2002 Published by Elsevier Science Ltd.
PII: S0042-207X(02)00327-5

coupled to the system of equations in Refs. [6,11]. Nevertheless, in all these works the kinetics of nitrogen atoms was simplified insofar as the kinetics of the atomic metastable species $N(^2D)$ and $N(^2P)$ was not included (it was simply assumed that most of the atomic metastables give back a ground-state atom $N(^4S)$ [10,11]). In particular, it was shown that the main reactions for the destruction of $N(^4S)$ atoms under discharge conditions at low pressures, namely

$$e + N(^4S) \rightarrow e + N(^2D), \quad (1)$$

$$e + N(^4S) \rightarrow e + N(^2P) \quad (2)$$

and

$$N(^4S) + N2(A) \rightarrow N2(X, 6 \leqslant v \leqslant 9) + N(^2P) \quad (3)$$

do not correspond to complete loss of ground-state atoms since $\sim$70–95% of the metastable atoms $N(^2D)$ and $N(^2P)$ so formed are converted back to $N(^4S)$. In this way, the detailed kinetics of the metastable atoms is essential to determine the concentration of ground-state $N(^4S)$ atoms.

It is worth noting that the kinetics of atomic metastables has been included in our models for DC discharges in [14,15]. However, this has essentially been done to close the system of equations, and the kinetics of these states was not considered or analysed in detail. Moreover, due to the low degree of ionization of DC discharges as compared to the microwave ones, the concentration of ground-state atomic nitrogen for the conditions of Refs. [14,15] is essentially dictated by the recombination probability of $N(^4S)$ atoms at the wall. On the contrary, for the high electron densities of the present work, reactions (1) and (2) are much more important than in the DC case and the kinetics of the atomic metastable states is strongly coupled to that of ground-state atoms.

In this work, we present a theoretical investigation of a nitrogen microwave discharge operating at wave frequency $\omega/(2\pi) = 2.45\,\text{GHz}$ and pressure $p = 2\,\text{Torr}$ ($\approx 267\,\text{Pa}$), in order to study the behaviour of metastable $N(^2D)$ and $N(^2P)$ atoms and of the molecular metastable $N_2(A^3\Sigma_u^+)$ as a function of the discharge operating and wall conditions. In the next section, we present the kinetic scheme used to describe these metastable states. The results are presented and discussed in Section 3, and Section 4 summarizes the main conclusions.

2. Kinetics of metastables

The volume kinetics of atoms excited in metastable states and their interactions with the wall have a significant influence on the dissociation processes in nitrogen. In order to reveal the coupling between these states and ground-state $N(^4S)$ atoms, pointed out in [10,11], we developed a self-consistent theoretical model to describe a nitrogen microwave discharge. The basic model has been described in previous articles [6,10,11,13], but here we have further included the rate balance equations for the atomic metastable species $N(^2D)$ and $N(^2P)$. In addition to the atomic metastable states, special attention is paid to the molecular metastable state $N_2(A\ ^3\Sigma_u^+)$ since its kinetics is coupled to that of the atomic species.

The complete set of equations and the various processes taken into account to determine the populations of the species $N_2(X\ ^1\Sigma_g^+, v)$, $N_2(A\ ^3\Sigma_u^+)$, $N_2(B\ ^3\Pi_g)$, $N_2(C\ ^3\Pi_u)$, $N_2(a'\ ^1\Sigma_u^-)$, $N_2(a\ ^1\Pi_g)$, $N_2(w\ ^1\Delta_u)$, $N_2(a''\ ^1\Sigma_g^+)$, $N(^4S)$, N_2^+ and N_4^+, as well as the choice of the corresponding rate coefficients, have been discussed in Refs. [6,10,11]. The list of the reactions involved in the kinetics of $N(^2D)$, $N(^2P)$, which was not considered before, is shown in Table 1. The different processes involved in the kinetics of $N_2(A\ ^3\Sigma_u^+)$ have been considered in Refs. [6,10,11], with the exception of reaction (R11). In Table 1, the symbol $f(E/N)$ is used for electron rate coefficients calculated from the electron Boltzmann equation.

In reactions (R12) and (R13) in Table 1 it is assumed that all the metastable atoms arriving at the discharge tube wall are destroyed. However, for these two reactions we will assume that a certain fraction δ of the metastable atoms are quenched to the ground-state $N(^4S)$, while the remaining fraction $1-\delta$ recombines into N_2 molecules. In our basic model we will (rather arbitrarily) consider $\delta = 0.5$. This assumption is questionable but the sensitivity of the results to

Table 1
Kinetics of the $N(^2D)$ and $N(^2P)$ atomic metastable states in a nitrogen discharge

	Process	Rate coefficient	Reference
R1	$e + N_2 \rightarrow e + N(^4S) + N(^2D)$	$f(E/N)$	[10]
R2	$e + N(^4S) \leftrightarrow e + N(^2D)$	$f(E/N)$	[19]
R3	$e + N(^4S) \leftrightarrow e + N(^2P)$	$f(E/N)$	[19]
R4	$e + N(^2D) \leftrightarrow e + N(^2P)$	$f(E/N)$	[19]
R5	$N(^2D) + N_2 \rightarrow N(^4S) + N_2$	$k = 10^{-13}\exp(-510/T_g)\,cm^3\,s^{-1}$	[20]
R6	$N(^2D) + N(^2P) \rightarrow N_2^+ + e$	$k = 10^{-13}\,cm^3\,s^{-1}$	[21]
R7	$N_2(A) + N(^4S) \rightarrow N_2(X, 6 \leqslant v \leqslant 9) + N(^2P)$	$k = 4 \times 10^{-11}\,cm^3\,s^{-1}$	[10]
R8	$N(^4S) + N(^2P) \rightarrow N(^4S) + N(^2D)$	$k = 6 \times 10^{-13}\,cm^3\,s^{-1}$	[21]
R9	$N(^4S) + N(^2P) \rightarrow N(^4S) + N(^4S)$	$k = 1.8 \times 10^{-12}\,cm^3\,s^{-1}$	[21]
R10	$N(^2P) + N_2 \rightarrow N(^4S) + N_2$	$k = 6 \times 10^{-14}\,cm^3\,s^{-1}$	[21]
R11	$N(^2P) + N_2(X, v \geqslant 10) \rightarrow N(^4S) + N_2(A)$	$k = 10^{-10}\exp(-1300/T_g)\,cm^3\,s^{-1}$	[21]
R12	Diffusion of $N(^2D)$ to the wall	$ND = 6.4 \times 10^{18}(T_g/300)^{0.5}\,cm^{-1}\,s^{-1}$	[22]
R13	Diffusion of $N(^2P)$ to the wall	$ND = 5.2 \times 10^{18}(T_g/300)^{0.5}\,cm^{-1}\,s^{-1}$	[22]

this parameter is checked by calculations for a different value of δ. The molecular metastable states are assumed to be quenched to ground-state $N_2(X)$ molecules with probability one. Note that in the gas thermal balance equation only half of the energy released by the deactivation of metastables at the wall is assumed to produce gas heating; half is considered to heat the wall [11].

3. Results and discussion

We now present the results obtained for a nitrogen surface-wave discharge at $f = 2.45\,GHz$, $p = 267\,Pa$, in a quartz tube of radius $R = 0.75\,cm$. The input parameters needed are the electron density at the launcher $n_{e0} = 1.2 \times 10^{12}\,cm^{-3}$ and the axial profile of the wall temperature, $T_w(z)$, which were taken from the experiment [13,16]. All the remaining quantities and the axial structure of the discharge are calculated from the model [11].

Fig. 1 shows the axial variation of the relative concentration of the species $N(^4S)$, $N(^2D)$, $N(^2P)$ and $N_2(A\ ^3\Sigma_u^+)$ assuming that half of the metastable atoms that reach the wall are deactivated to the ground-state $N(^4S)$ (i.e., $\delta = 0.5$). The axial position is normalized to the total discharge length, L_T, in such a way that $\Delta z/L_T = 1$ corresponds to the position of the launcher and $\Delta z/L_T = 0$ to the plasma column end. The relative concentrations of the species decrease towards the column end, essentially as a consequence of the decrease in the electron density along the discharge [13].

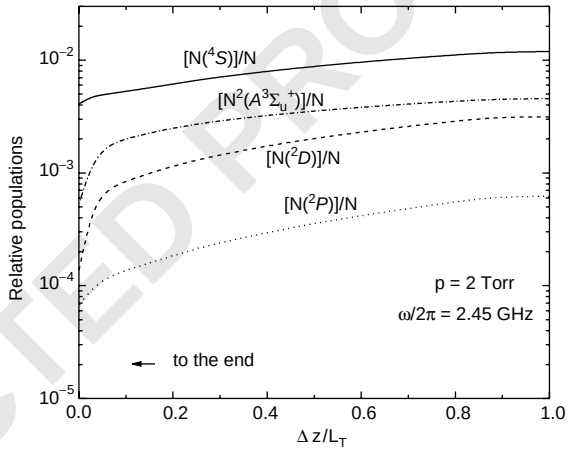

Fig. 1. Relative concentration of the species $N(^4S)$ (—), $N(^2D)$ (– –), $N(^2P)$ (…) and $N_2(A\ ^3\Sigma_u^+)$ (–.–) along the discharge.

The exact contribution of each reaction to the creation and destruction of $N(^4S)$ atoms can be evaluated from Figs. 2 and 3. Fig. 2 shows the contribution of the different destruction channels of ground-state atoms: recombination at the wall, $e + N(^4S) \rightarrow (1/2)N_2$ (full curve); electron impact destruction by reaction R2, $e + N(^4S) \rightarrow e + N(^2D)$ (broken curve); electron impact destruction by reaction R3, $e + N(^4S) \rightarrow e + N(^2P)$ (dotted curve);

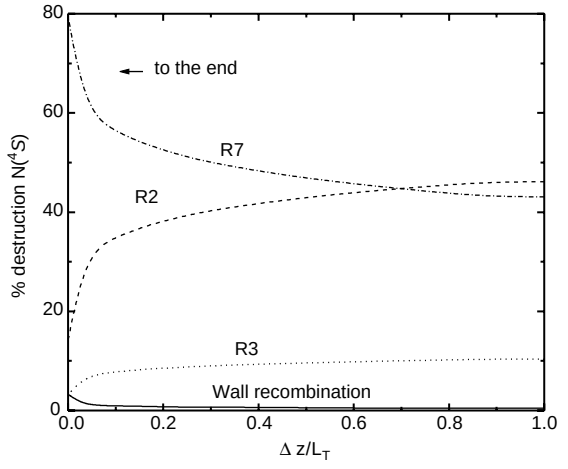

Fig. 2. Percentage contributions of the various destruction processes of $N(^4S)$ atoms along the discharge: $N(^4S)+\text{Wall}\rightarrow(1/2)N_2(X, v=0)$ (—); reaction R2 (– –); R3 (…); R7 (–.–).

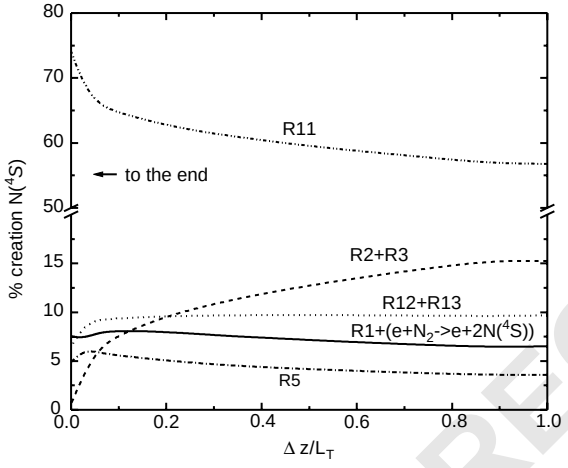

Fig. 3. Percentage contributions of the various creation processes of $N(^4S)$ atoms along the discharge: dissociation of N_2 by electron impact, $e+N_2\rightarrow N(^4S)+N(^4S)$ and $e+N_2\rightarrow N(^4S)+N(^2D)$ (—); reactions R2 and R3 (– –); R12 and R13 (…); R5 (–.–); R11 (..–).

and destruction in collisions with the metastable state $N_2(A\ ^3\Sigma_u^+)$ through reaction R7, $N_2(A)+N(^4S)\rightarrow N_2(X, 6\leqslant v\leqslant 9)+N(^2P)$ (chain curve). Close to the launcher, where the electron density is higher, the destruction processes by electron impact dominate, especially reaction R2. However, as we move along the discharge axis towards the plasma column end, reaction R7 involving metastable molecules $N_2(A)$ starts to dominate. Destruction of $N(^4S)$ atoms at the wall seems to be a minor loss channel. Nevertheless, we must keep in mind the uncertainties in the collisional data, in particular in the value of the recombination probability of nitrogen atoms at the wall, γ_N. Here, we considered $\gamma_N = 5\times10^{-4}$ [17]. A larger value of γ_N would lead to a higher contribution of wall losses. On the other hand, reactions (R2), (R3) and (R7) do not destroy effectively ground-state $N(^4S)$ atoms, since most of the metastable atoms formed in these reactions give back $N(^4S)$ atoms as shown in Fig. 3. This figure presents the percentage contribution of the different creation reactions of $N(^4S)$ atoms: dissociation of N_2 by electron impact, $e+N_2\rightarrow N(^4S)+N(^4S)$ and $e+N_2\rightarrow N(^4S)+N(^2D)$ (full curve); electron superelastic collisions with $N(^2D)$ and $N(^2P)$, $e+N(^2D,^2P)\rightarrow e+N(^4S)$, reactions R2 and R3 (broken curve); deactivation of metastable atoms at the wall, $N(^2D,^2P)+\text{wall}\rightarrow N(^4S)$, R12 and R13 (dotted curve); quenching of $N(^2D)$ by N_2 molecules, $N(^2D)+N_2\rightarrow N(^4S)+N_2$, reaction R5 (chain curve); quenching of $N(^2P)$ by vibrationally excited molecules, $N(^2P)+N(X, v\geqslant10)\rightarrow N(^4S)+N_2(A)$, R11 (double chain curve). Other processes not shown in this figure, such as vibrational dissociation, have a contribution always $<2\%$. Fig. 3 clearly shows that the main creation mechanisms of ground-state atoms involve the metastable species $N(^2D)$ and $N(^2P)$, so that reactions (R2), (R3) and (R7) do not constitute full destruction mechanisms for $N(^4S)$ atoms. From the model we calculate that $\approx90\%$ of the created metastable atoms give back $N(^4S)$. This confirms the assumptions made in Refs. [10,11], where a simplified kinetics for the metastable atoms was considered. We can further conclude that the kinetics of the three atomic species is strongly coupled, and that mechanisms with relatively low importance for the creation or the destruction of one of these species may significantly influence the other species. For example, (R7) is the main reaction for the destruction of $N(^4S)$ but it is practically cancelled by the reverse reaction (R11) which constitutes the main source of ground-state atoms. These two

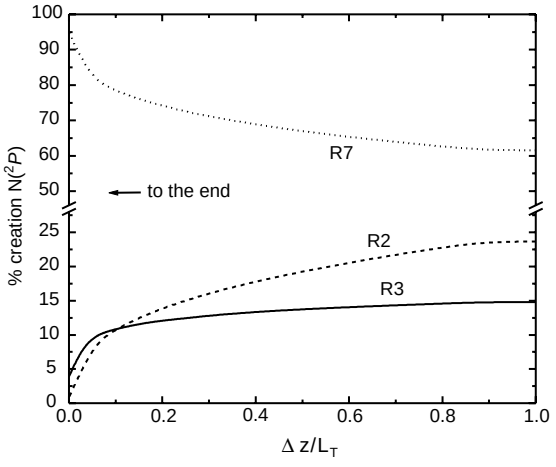

Fig. 4. Percentage contributions of the various creation processes of N(^{2}P) atoms along the discharge: electron impact excitation of N(^{4}S), reaction R3 (—); electron impact excitation of N(^{2}D), reaction R2 (– –); reaction R7 (…).

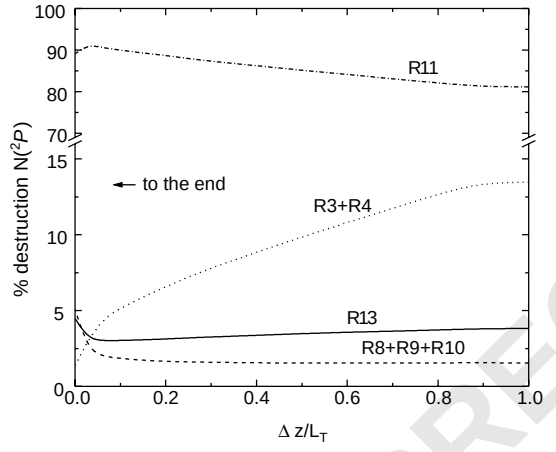

Fig. 5. Percentage contributions of the various destruction processes of N(^{2}P) atoms along the discharge: destruction at the wall, reaction R13 (—); quenching with N(^{4}S) and N_2, reactions R8–R10 (– –); destruction by electron impact, R3 and R4 (…); R11 (–.–).

reactions ensure a strong correlation between the atom kinetics and that of $N_2(A\ ^3\Sigma_u^+)$. This can further be confirmed in Figs. 4 and 5, where we present the creation and destruction mechanisms of N(^{2}P) metastable atoms.

As expected, the contribution of the electronic processes decreases towards the column end due to the decrease in electron density. Reaction (R7) is by far the main reaction for the formation of N(^{2}P) while reaction (R11) is the dominant destruction process. However, these two reactions contribute always less than 5% to the destruction/creation of the state $N_2(A\ ^3\Sigma_u^+)$ due to the coupling between this state and the state $N_2(B\ ^3\Pi_g)$ [6,10].

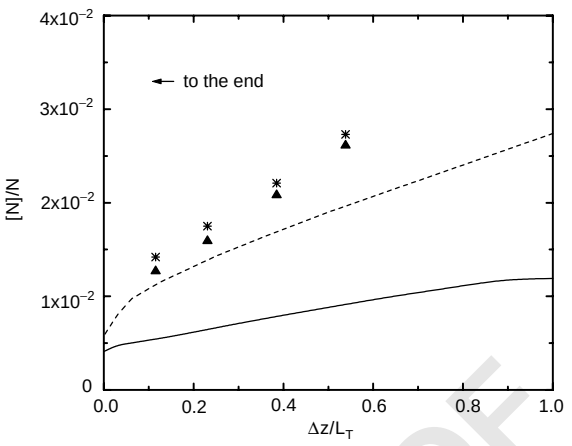

Fig. 6. Relative concentration of N(^{4}S): experimental measurements from [16] (□,); calculations from the basic model (—) and assuming $\delta = 0.8$ (– –).

In order to check the influence of the parameter δ on the results, Fig. 6 shows the calculated relative concentration of ground-state atoms both from our basic model and assuming $\delta = 0.8$. This figure also presents the atomic concentration measured by actinometry [18] for the same conditions as in the calculations [16]. The two series of points correspond to the values obtained using the emission of two different atomic lines of nitrogen, namely at $\lambda = 746.83$ and 744.23 nm. The actinometry technique provides the absolute measurements indicated in Fig. 6, but it should be kept in mind that this technique is best suited for relative measurements. Therefore, the agreement between calculations and measurements can be considered good in both cases, even if the experimental values obtained are closer to the case $\delta = 0.8$. Work is in progress to apply the model to lower values of pressure, where diffusion of metastables to the wall is more important and thus the value of δ should play a more crucial role

than for the relatively high value of pressure of this work.

4. Conclusions

In the present study we developed an investigation of the kinetics of metastable atoms $N(^2D)$ and $N(^2P)$ by using a theoretical model based on the self-consistent treatment of electron and heavy-particle kinetics, wave electrodynamics and gas thermal balance. For the conditions considered, corresponding to a low-pressure nitrogen microwave discharge at $\omega/2\pi = 2.45\,\mathrm{GHz}$ and $p = 267\,\mathrm{Pa}$, the results demonstrate the existence of strong correlation between the kinetics of $N(^4S)$, $N(^2D)$ and $N(^2P)$ atoms and $N_2(A\ ^3\Sigma_u^+)$ metastables through reactions $e + N(^4S) \leftrightarrow e + N(^2D)$, $e + N(^4S) \leftrightarrow e + N(^2P)$, $N(^4S) + N_2(A\ ^3\Sigma_u^+) \rightarrow N_2(X, 6 \leqslant v \leqslant 9) + N(^2P)$ and $N_2(X, v \geqslant 10) + N(^2P) \rightarrow N(^4S) + N_2(A\ ^3\Sigma_u^+)$. Since the metastable state $N_2(A\ ^3\Sigma_u^+)$ is involved in different fundamental processes of the discharge such as ionisation, gas heating and population of the vibrational levels of electronic ground-state molecules [6], it is of paramount importance to understand the mechanisms determining the population of this state and of the atomic species in detail.

Acknowledgements

The authors want to express their gratitude to Dr. J. Loureiro for very fruitful discussions.

References

[1] Loureiro J, Sá PA, Guerra V. J Phys D: Appl Phys 2001;34:1769.
[2] Sadeghi N, Foissac C, Supiot P. J Phys D: Appl Phys 2001;34:1769.
[3] Dillece G, Simek M, de Benedictis S. J Phys D: Appl Phys 2001;34:1799.
[4] Krames TG-MB, Meichsner J. J Phys D: Appl Phys 2001;34:1799.
[5] Colonna G, Capitelli M. J Phys D: Appl Phys 2001;34:1812.
[6] Guerra V, Sá PA, Loureiro J. J Phys D: Appl Phys 2001;34:1745.
[7] Petrović ZL, Marković VL, Pejović MM, Gocić SR. J Phys D: Appl Phys 2001;34:1756.
[8] Camps E, Muhl S, Alvarez-Fregosz O, Islas JAJ, Olea O, Romero S. J Vac Sci Technol 1999;17:2007.
[9] Duez N, Mutel B, Dessaux O, Goudmand P, Grimblot J. Surf Coat Technol 2000;125:79.
[10] Guerra V, Loureiro J. Plasma Sources Sci Technol 1997;6:361.
[11] Guerra V, Tatarova E, Dias FM, Ferreira CM. J Appl Phys 2002;91\par.
[12] Guerra V, Loureiro J. Plasma Sources Sci Technol 1999;8:110.
[13] Tatarova E, Dias FM, Ferreira CM, Ricard A. J Appl Phys 1999;85:49.
[14] Gordiets BF, Ferreira CM, Guerra VL, Loureiro JMAH, Nahorny J, Pagnon D, Touzeau M, Vialle M. IEEE Trans Plasma Sci 1995;23:750.
[15] Gordiets BF, Ferreira CM, Pinheiro MJ, Ricard A. Plasma Sources Sci Technol 1998;7:363.
[16] Tatarova E, Guerra V, Dias FM, Ferreira CM. In: Proceedings of the 15th International Symposium on Plasma Chemistry. France: Orléans, 2001. p. 2263–8.
[17] Kim YC, Boudart M. Langmuir 1991;7:2999.
[18] Thomaz JC, Amorim J, Souza CF. J Phys D: Appl Phys 1999;32:3208.
[19] Berrington KA, Burke PG, Robb WB. J Phys B: At Mol Phys 1975;8:2500.
[20] Black TG. J Chem Phys 1976;64:4442.
[21] Vereshchagin KA, Smirnov VV, Shakhatov VA. Tech Phys 1997;42:487.
[22] Cernogora G. Ph.D. thesis, Université de Paris-Sud, Orsay-France, 1980.